

High Selectively C₂H₄/C₂H₂ Separation by cyano-functionalized alkadiyne-pyrene conjugated frameworks membrane

Jie Liu,^{a‡} Junjie Chen,^{a‡} Guosheng Shi,^a Junjie Hao,^a Caiyuan Wu,^a Yuqing Liu,^a Xu Zhao^a and Xing Liu^{a*}

^aShanghai Key Laboratory of Atomic Control and Application of Inorganic 2D Supermaterials, Shanghai Applied Radiation Institute, Shanghai University, Shanghai 200444, China.

*Corresponding authors: liuxing0215@shu.edu.cn (X.L.)

‡These authors contributed equally to this work.

PS1: The OPLS-AA force-field parameters for PTEP, CN-PTEP, gas molecules, and graphene.

PS2: Definition of C-H...N hydrogen bonding and analysis of the most stable adsorption configurations of C₂H₄ and C₂H₂ on CN-PTEP.

PS3: Other adsorption configurations and adsorption energies of gas molecules on the CN-PTEP and PTEP membranes.

PS4: Transition-state interaction analysis for C₂H₄ and C₂H₂ permeation through the CN-PTEP pore.

PS5: The estimation of pre-exponential factors for C₂H₄ and C₂H₂ based on transition-state theory.

PS6: Effect of ESP-derived pore-edge charges on the MD permeation results.

PS7: MD simulation model and the permeation behavior of the pristine PTEP membrane.

PS1: The OPLS-AA force-field parameters for PTEP, CN-PTEP, gas molecules, and graphene.

The PTEP and CN-PTEP membranes were described within the OPLS-AA framework, in which membrane atoms were assigned Lennard-Jones (LJ) parameters and partial charges according to their local chemical environments. As shown in Fig. S1a-b and Table S1, the pristine PTEP membrane contains one labeled hydrogen site (H) and three labeled carbon sites (C1, C2, and C3). Specifically, H denotes the hydrogen atom attached to the benzene ring, C1 refers to the carbon atom in the benzene ring bonded to H, C2 denotes a carbon atom in the benzene ring, and C3 denotes a carbon atom in the alkynyl chain. For the CN-functionalized membrane, N1 denotes the nitrogen atom in the -CN group, C1 denotes the carbon atom in the -CN group, C2 denotes the carbon atom in the benzene ring directly bonded to the -CN group, C3 denotes a carbon atom in the benzene ring, and C4 denotes a carbon atom in the alkynyl chain. The gas molecules C_2H_2 and C_2H_4 were also described using the OPLS-AA force field, and the corresponding parameters are summarized in Table S1.

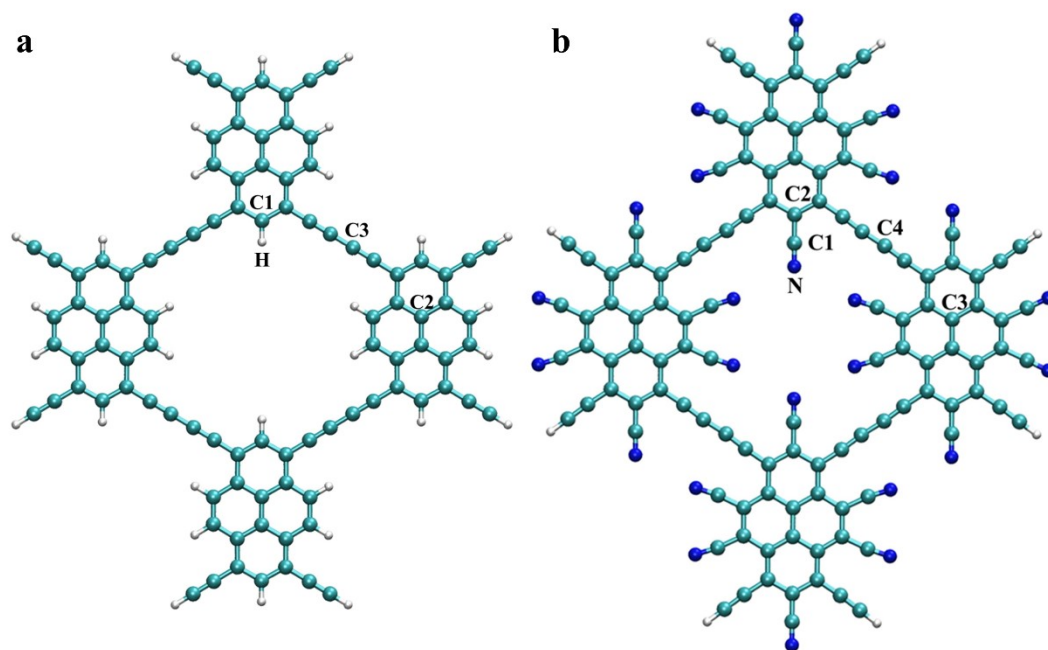


Fig. S1 Atom-type assignment for the PTEP and CN-PTEP membranes. Atoms are colored as follows: C, cyan; H, white; N, blue.

Table R1. The OPLS-AA force-field parameters used for PTEP, CN-PTEP, C₂H₂, and C₂H₄ in the MD simulations.

Molecule	Atom type	ϵ (kJ/mol)	σ (Å)	q(e)	Ref
PTEP	C1	0.293	3.550	-0.115	1
	C2	0.293	3.550	0.000	1
	C3	0.360	3.400	0.000	2
	H	0.126	2.420	0.115	1
CN-PTEP	C1	0.628	3.650	0.395	3
	C2	0.293	3.550	0.035	3
	C3	0.293	3.550	0.000	1
	C4	0.360	3.400	0.000	2
C₂H₂	N	0.711	3.200	-0.430	3
	C	0.360	3.300	-0.294	4
	H	0.063	2.420	0.294	4
C₂H₄	C	0.318	3.550	-0.330	4
	H	0.126	2.420	0.165	4
graphene	C	0.293	3.400	0.000	5

PS2: Definition of C-H \cdots N hydrogen bonding and analysis of the most stable adsorption configurations of C₂H₄ and C₂H₂ on CN-PTEP.

According to previous studies^{6, 7} and the IUPAC⁸ recommendation, a C-H \cdots N interaction can be considered to form hydrogen bond when the H \cdots N distance is within the sum of the van der Waals radii of H and N and the C-H \cdots N angle is larger than 110°. For the present system, we therefore considered the H \cdots N distances and the \angle C-H \cdots N angles between C₂H₄/C₂H₂ and the cyano functional groups inside the pore. Using the commonly adopted van der Waals radii of 1.20 Å for H and 1.55 Å for N, the corresponding H \cdots N distance is 2.75 Å.

As shown in Fig. S2, for the most stable adsorption configuration of C₂H₄ adsorption on the CN-PTEP membrane, the H1 \cdots N1 distance was 2.46 Å and the angle \angle C1-H1 \cdots N1 was 162.4°, the H2 \cdots N2 distance was 2.41 Å and the angle \angle C1-H2 \cdots N2 angle was 174.6°, which indicate two C-H \cdots N hydrogen bonds formed between C₂H₄ and CN-PTEP. In contrast, for the most stable adsorption configuration of C₂H₂ adsorption on the CN-PTEP membrane, the H1 \cdots N1 and H1 \cdots N2 distances increase to 3.57 and 3.47 Å, respectively, while the corresponding \angle C1-H1 \cdots N1 and \angle C1-H1 \cdots N2 angles decrease to 111.8° and 113.8°, which indicates C₂H₂ cannot form C-H \cdots N hydrogen bond with CN-PTEP membrane.

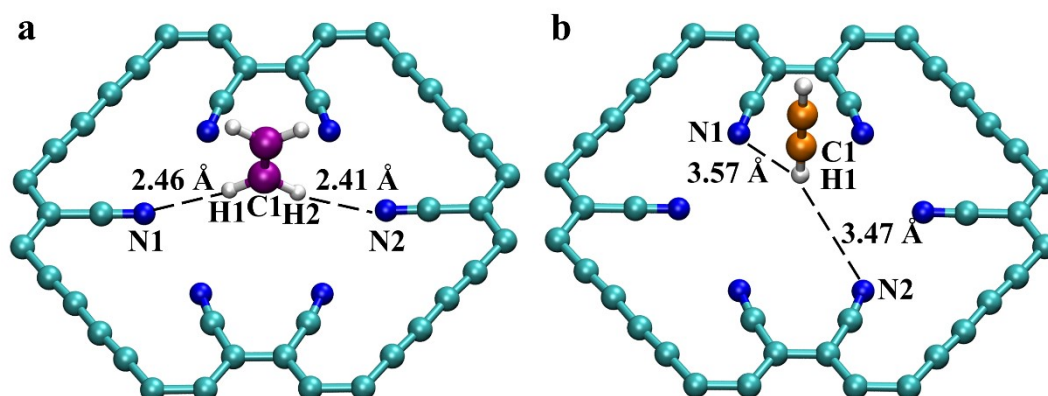


Fig. S2 Optimized configurations of C₂H₄ and C₂H₂ adsorption on the CN-PTEP membrane. Atoms are colored as follows: C, cyan; H, white; N, blue. For clarity, the carbon atoms of C₂H₄ are colored purple, and the carbon atoms of C₂H₂ are colored orange.

PS3: Other adsorption configurations and adsorption energies of gas molecules on the CN-PTEP and PTEP membranes.

Fig. S3 shows the different adsorption configurations of ethylene (C_2H_4) and acetylene (C_2H_2) molecules on the CN-PTEP membrane, where d represents the perpendicular distance of the gas molecules from the membrane surface.

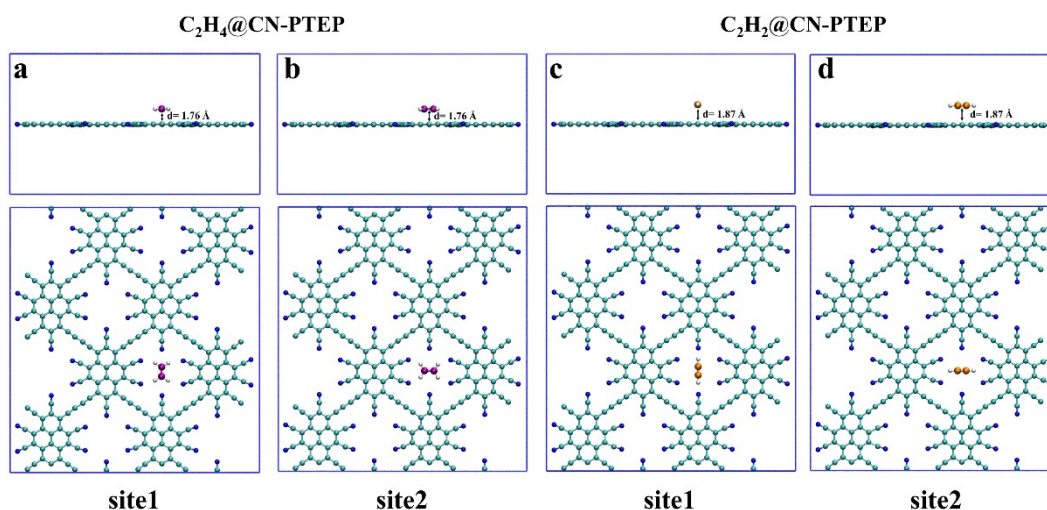


Fig. S3 Adsorption configuration of C_2H_4 and C_2H_2 on CN-PTEP membrane. The different adsorption configurations of C_2H_4 molecules (a-b) and C_2H_2 molecules (c-d) on CN-PTEP membranes, as well as their vertical heights relative to the membrane surface. Atoms are colored as follows: C, cyan; H, white; N, blue. For clarity, the carbon atom of C_2H_4 is colored purple, and the carbon atom of C_2H_2 is colored orange.

As shown in Fig. S4, the most stable adsorption configuration of C_2H_4 was oriented horizontally at the center of the membrane pore (Fig. S4a), while C_2H_2 was adsorbed vertically at the pore center and aligned perpendicular to the PTEP membrane plane (Fig. S4i).

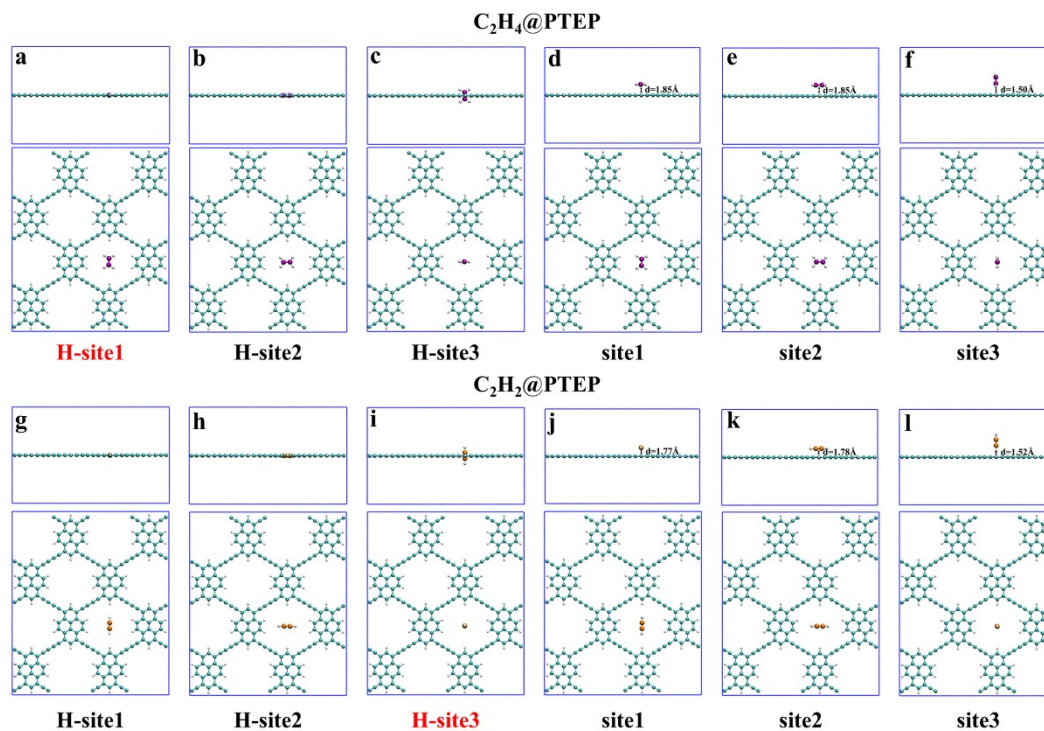


Fig. S4 Adsorption configuration of C_2H_4 and C_2H_2 on PTEP membrane. The different adsorption configurations of acetylene molecules (a-f) and ethylene molecules (g-l) on PTEP membranes, as well as their vertical heights relative to the membrane surface. Atoms are colored as follows: C, cyan; H, white; N, blue. For clarity, the carbon atom of C_2H_4 is colored purple, the carbon atom of C_2H_2 is colored orange.

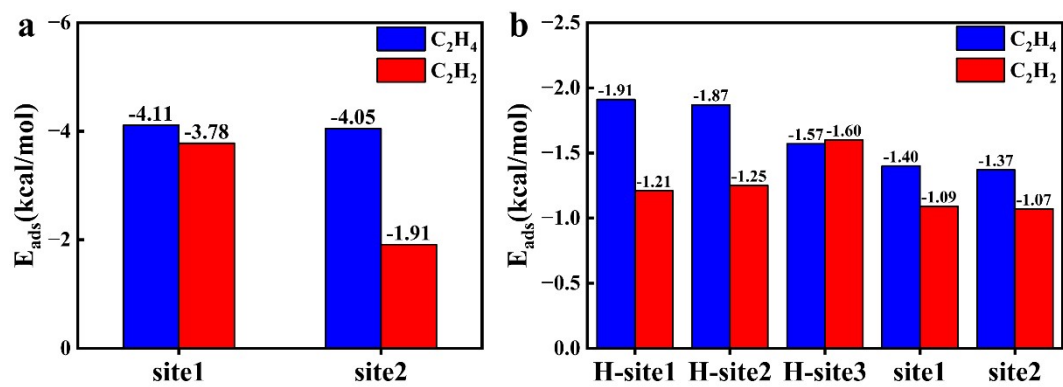


Fig. S5 Adsorption energies of C₂H₄ and C₂H₂ on CN-PTEP and PTEP membranes with different adsorption configurations. (a) Adsorption energies on the CN-PTEP membrane;(b) Adsorption energies on the pristine PTEP membrane.

PS4: Transition-state interaction analysis for C₂H₄ and C₂H₂ permeation through the CN-PTEP pore.

We further analyzed the transition-state geometries and pore-molecule interactions in detail. The pore-molecule interaction at the transition state was defined as follows:

$$E_{\text{int}} = E_{\text{TS}} - E_{\text{CN-PTEP}} - E_{\text{gas}}$$

where E_{TS} is the total energy of the transition-state configuration, $E_{\text{CN-PTEP}}$ is the energy of the CN-PTEP membrane, and E_{gas} is the energy of the gas molecules.

The interaction energy between C₂H₄ and CN-PTEP at the TS is -4.09 kcal/mol, this attraction interaction mainly results from the C-H \cdots N hydrogen bond formed between C₂H₄ and CN-PTEP, thus the energy barrier of C₂H₄ is very small. Whereas the interaction of C₂H₂ is 2.63 kcal/mol, which shows that C₂H₂ was repelled when passing through the pore, thus the relatively high energy barrier needs to be overcome.

As shown in Fig. R5, the H1 \cdots N1 distance was 2.44 Å and the angle \angle C1-H1 \cdots N1 was 134.3°, and the H2 \cdots N2 distance was 2.44 Å and the angle \angle C1-H2 \cdots N2 angle was 137.4°, which indicates two C-H \cdots N hydrogen bonds formed between C₂H₄ and CN-PTEP. In contrast, for C₂H₂, the H1 \cdots N1 and H1 \cdots N2 distances increase to 3.63 and 3.72 Å, respectively, while the corresponding \angle C1-H1 \cdots N1 and \angle C1-H1 \cdots N2 angles decrease to 64.7° and 63.6°, which indicates C₂H₂ cannot form C-H \cdots N hydrogen bond with the CN-PTEP membrane. C₂H₄ formed two C-H \cdots N hydrogen bonds with the CN-PTEP membrane, which results in the favorable orientation of C₂H₄ to pass through the nanopore of CN-PTEP. However, C₂H₂ without C-H \cdots N hydrogen bond passes vertically through the nanopore of the CN-PTEP. These results showed that the selective permeation of C₂H₄ arises from the C-H \cdots N hydrogen-bonding interaction and the resulting favorable orientational.

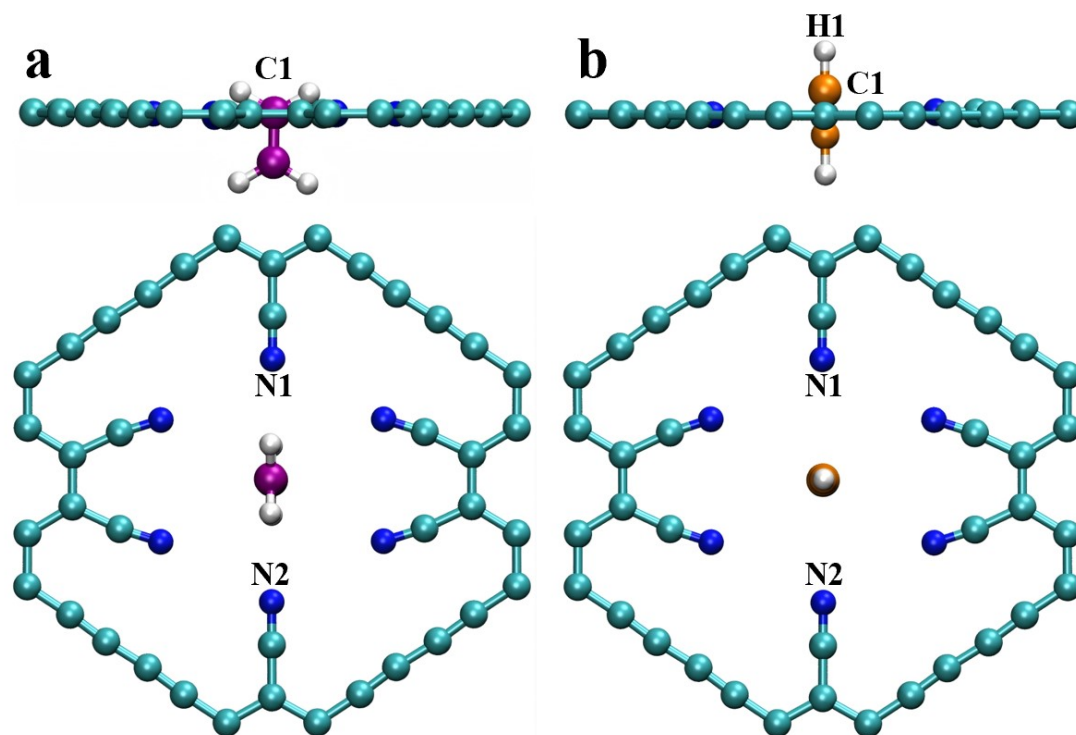


Fig. S6 Transition-state configurations of C_2H_4 and C_2H_2 permeation through the CN-PTEP pore. Atoms are colored as follows: C, cyan; H, white; N, blue. For clarity, the carbon atoms of C_2H_4 are colored purple, and the carbon atoms of C_2H_2 are colored orange.

PS5: The estimation of pre-exponential factors for C₂H₄ and C₂H₂ based on transition-state theory.

We have performed vibrational frequency analyses for both the initial states (IS) and transition states (TS) of C₂H₄ and C₂H₂ permeation, and estimated the pre-exponential factors based on the transition-state theory (TST). According to the previous research⁹, the pre-exponential factor was calculated as follows:

$$A_{\text{act}} = \frac{k_{\text{B}}T}{h} \exp\left(\frac{\Delta S^{\ddagger}}{k_{\text{B}}}\right) \quad (4)$$

where k_{B} is the Boltzmann constant, T is the temperature, h is the Planck constant, ΔS^{\ddagger} is the activation entropy defined as $S_{\text{TS}} - S_{\text{IS}}$.

Table S2 The pre-exponential factors based on TST, diffusion barriers, and corrected ideal selectivity for C₂H₄/C₂H₂ permeation through the CN-PTEP membrane at 298 K.

gas	A (s ⁻¹)	E _b (kcal/mol)	selectivity
C ₂ H ₄	4.15×10 ¹²	0.87	1×10 ⁴
C ₂ H ₂	1.05×10 ¹³	6.87	

PS6: Effect of ESP-derived pore-edge charges on the MD permeation results.

To assess the possible influence of the pore-edge electrostatic environment on the MD results, we further examined the effect of ESP-derived charges for representative pore-edge atoms in the CN-PTEP membrane. The original MD simulations were carried out using the charge parameters provided by the OPLS-AA force field. To refine the electrostatic description around the pore edge, a representative cluster model of the CN-PTEP pore region was constructed, as shown in Fig. S7a. Based on this cluster model, DFT calculations were performed using Gaussian¹⁰ at the B3LYP/6-31G(d) level¹¹, and the electrostatic potential (ESP) charges of the key pore-edge atoms were subsequently obtained using the Multiwfn program¹².

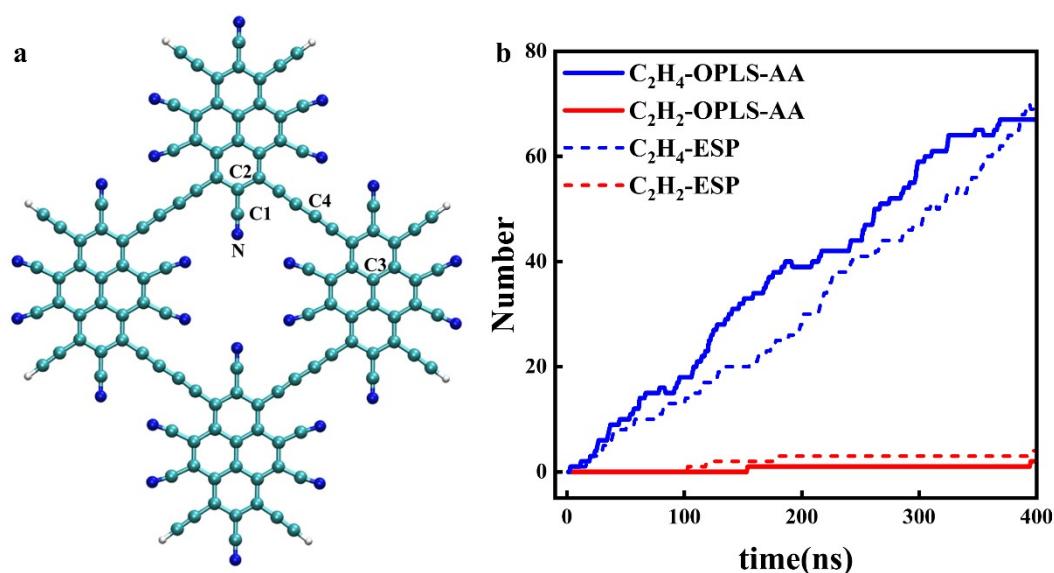


Fig. S7 ESP charge derivation and MD validation for the CN-PTEP pore. (a) Representative cluster model of the CN-PTEP pore used for DFT-based ESP charge analysis. N1 denotes the nitrogen atom in the -CN group, C1 denotes the carbon atom in the -CN group, C2 denotes the carbon atom in the benzene ring bonded to the -CN group, C3 denotes a carbon atom in the benzene ring, and C4 denotes a carbon atom in the alkyne chain. (b) Time evolution of permeated molecule numbers at 298 K obtained using the original OPLS-AA charges (solid lines) and the ESP-derived charges (dashed lines). Atoms are colored as follows: C, cyan; H, white; N, blue.

The resulting ESP-derived charges were compared with the original charge

parameters used in the MD simulations, and the detailed comparison is summarized in Table S3. For the representative pore-edge atoms, the original/ESP-derived charges are 0.395/0.382 for C1, 0.035/0.023 for C2, 0/0 for C3, 0/0 for C4, and -0.430/-0.405 for N, respectively. Although the absolute magnitudes are slightly reduced in the ESP-derived values, the charge signs and the relative electrostatic distribution around the pore are consistent.

To further evaluate whether this charge difference would affect the MD results, we further performed a validation simulation at 298 K by using the ESP-derived charges. As shown in Fig. S7b, compared with the original charge set, the number of permeated C_2H_4 molecules changed only slightly from 67 to 70, while that of C_2H_2 changed from 2 to 4 after the same 400 ns simulation time. Thus, the use of ESP-derived charges leads to minor quantitative variations and does not alter the qualitative permeation trend. In particular, CN-PTEP still exhibits a pronounced preferential permeation for C_2H_4 over C_2H_2 .

Table S3 Original and ESP-derived charges of the key pore-edge atoms in CN-PTEP

Atom	C1	C2	C3	C4	N
OPLS-AA charge	0.395	0.035	0.000	0.000	-0.430
ESP-derived charge	0.382	0.023	0.000	0.000	-0.405

PS7: MD simulation model and the permeation behavior of the pristine PTEP membrane.

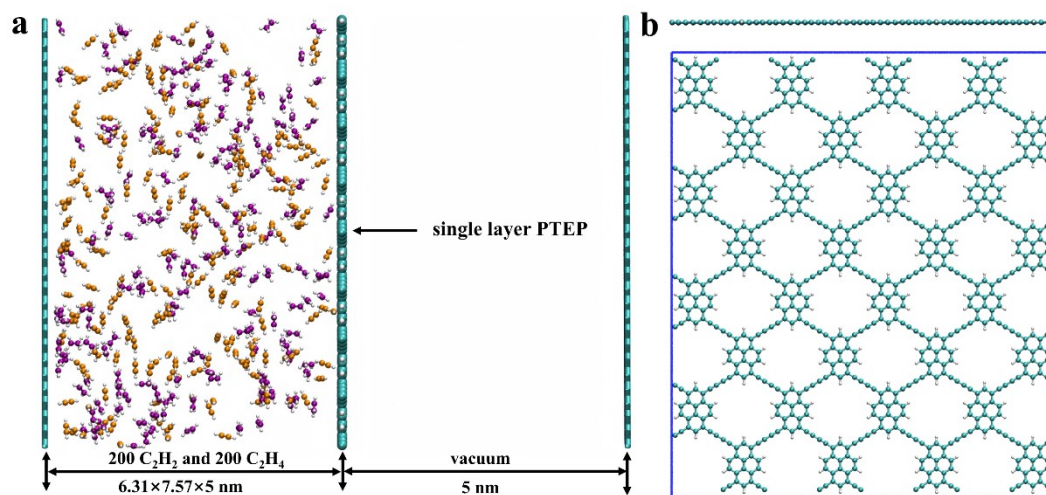


Fig. S8 MD simulation model and PTEP membrane structure for C₂H₄/C₂H₂ separation.

(a) Simulation model of the C₂H₄/C₂H₂ mixture separation through the PTEP membrane. (b) Side and top views of the single-layer PTEP used in the simulations. Atoms are colored as follows: C, cyan; H, white. For clarity, the carbon atoms of C₂H₄ are colored purple, the carbon atoms of C₂H₂ are colored orange.

Fig. S9a showed the variation of the number of C_2H_4 and C_2H_2 passing through the PTEP membrane over time. Fig. S9b was a snapshot of the separation system at 500 ps. At this time, ~ 101 C_2H_2 and ~ 99 C_2H_4 pass through the PTEP membrane.

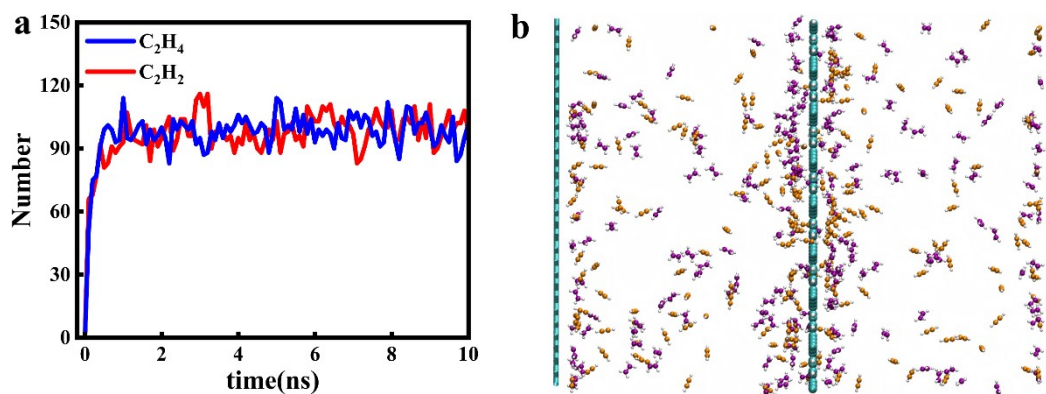


Fig. S9 Separation performance of the CN-PTEP membrane for C_2H_4/C_2H_2 . (a) The number of gas molecules passing through the PTEP membrane changed with simulation time. (b) Snapshots of the C_2H_4/C_2H_2 gas mixtures permeating through the PTEP membrane after 500 ps. Atoms are colored as follows: C, cyan; H, white. For clarity, the carbon atoms of C_2H_4 are colored purple, the carbon atoms of C_2H_2 are colored orange.

References

- 1 F. Müller-Plathe, *Macromolecules*. 1996, 29, 4782-4791.
- 2 X. Zheng, S. Ban, B. Liu, G. Chen, *Chin. J. Chem. Eng.* 2020, 28, 1898-1903.
- 3 M.L. Price, D. Ostrovsky, W.L. Jorgensen, *J. Comput. Chem.* 2001, 22, 1340-1352.
- 4 H. Xing, X. Zhao, Q. Yang, B. Su, Z. Bao, Y. Yang, Q. Ren, *Ind. Eng. Chem. Res.* 2013, 52, 9308-9316.
- 5 N. Karimzadeh, J. Azamat, H. Erfan-Niya, *J. Mol. Graph. Model.* 2022, 110, 108059.
- 6 R. Taylor, O. Kennard, *J. Am. Chem. Soc.* 1982, 104, 5063-5070.
- 7 S.J. Grabowski, *Chem. Commun.* 2024, 60, 6239-6255.
- 8 E. Arunan, G.R. Desiraju, R.A. Klein, J. Sadlej, S. Scheiner, I. Alkorta, D.C. Clary, R.H. Crabtree, J.J. Dannenberg, P. Hobza, *Pure Appl. Chem.* 2011, 83, 1637-1641.
- 9 Z. Yuan, G. He, S.X. Li, R.P. Misra, M.S. Strano, D. Blankschtein, *Adv. Mater.* 2022, 34, 2201472.
- 10 M. Frisch, G. Trucks, H. Schlegel, G. Scuseria, M. Robb, J. Cheeseman, G. Scalmani, V. Barone, G. Petersson, H. Nakatsuji, Wallingford, CT. 2016.
- 11 X. Li, M.J. Frisch, *J. Chem. Theory Comput.* 2006, 2, 835-839.
- 12 T. Lu, F. Chen, *J. Comput. Chem.* 2012, 33, 580-592.